Geophysical Prospecting

EAGE EUROPEAN ASSOCIATION OF GEOSCIENTISTS & ENGINEERS

Geophysical Prospecting doi: 10.1111/j.1365-2478.2012.01091.x

Poro-acoustoelasticity of fluid-saturated rocks

Jing Ba[1,3*], José M. Carcione[2], Hong Cao[1,3], Fengchang Yao[1,3] and Qizhen Du[4]

[1]*Research Institute of Petroleum Exploration & Development, PetroChina, Beijing, China,* [2]*Istituto Nazionale di Oceanografia e di Geofisica Sperimentale (OGS), Borgo Grotta Gigante 42c, 34010 Sgonico, Trieste, Italy,* [3]*Key Laboratory of Geophysics, PetroChina, Beijing, China, 100083, and* [4]*College of Geo-resources and Information, China University of Petroleum (East China), Dongying 257061, China*

Received May 2011, revision accepted February 2012

ABSTRACT

We generalize the classical theory of acoustoelasticity to the porous case (one fluid and a solid frame) and finite deformations. A unified treatment of non-linear acoustoelasticity of finite strains in fluid-saturated porous rocks is developed on the basis of Biot's theory. A strain-energy function, formed with eleven terms, combined with Biot's kinetic and dissipation energies, yields Lagrange's equations and consequently the wave equation of the medium. The velocities and dissipation factors of the P- and S-waves are obtained as a function of the 2nd- and 3rd-order elastic constants for hydrostatic and uniaxial loading. The theory yields the limit to the classical theory if the fluid is replaced with a solid with the same properties of the frame. We consider sandstone and obtain results for open-pore jacketed and closed-pore jacketed 'gedanken' experiments. Finally, we compare the theoretical results with experimental data.

Key words: Acoustoelasticity, Non-linearity, Waves, Porous media, Rock.

INTRODUCTION

The linear elastic theory of a single-phase medium is not suitable to describe the non-linear acoustic behaviour of realistic media, such as rocks, subject to loading stresses. Non-linear theories, based on 3rd-order elastic constants (3oEC), have been developed under the name of hyperelasticity (Truesdell 1965) and acoustoelasticity. These theories describe the behaviour of a medium subject to small dynamic motions (waves) and large static deformations (loading). Additional stiffness moduli affect wave velocities depending on the applied stress or strain.

Early works are those of Murnaghan (1937, 1951), Hearmon (1953), Goldberg (1961) and Hughes and Kelly (1953). The theory was well established by Toupin and Bernstein (1961), Jones and Kobett (1963) and Thurtson and Brugger (1964). Truesdell (1961) used four 3oEC. Brugger (1964) provided the thermodynamic definition of high-order elastic constants. Green (1973) collected measurements of 3oEC for various crystals and identified the notation of 3oEC defined by different authors. Grinfeld and Norris (1996) generalized the theory from single-phase to multi-phase materials.

The non-linear elasticity theory has been applied to rock mechanics (Johnson and Shankland 1989; Meegan et al. 1993). Winkler and Liu (1996) measured 3oEC in a variety of dry rocks and interpreted the results on the basis of the classical acoustoelasticity theory. They found that this theory successfully describes the relation between wave velocities and stress. However, similar experiments performed on water-saturated rocks showed that the classical 3oEC theory cannot fully describe the stress dependence of velocities (Winkler and McGowan 2004). The deformation of the fluid must be taken into account as the confining pressure increases.

Biot (1956) derived two-phase wave equations on the basis of the linear-elasticity theory, where the coupling between the solid and fluid is taken into account. Extensions of Biot's theory, to include fluid unrelaxation, are based on local fluid flow, dynamic permeability and multi-scale heterogeneity (Dutta and Odé 1979a,b; Johnson 2001; Berryman

* E-mail: baj04@mails.tsinghua.edu.cn, baj08@petrochina.com.cn

and Wang 2001; Pride, Berryman and Harris 2004; Carcione and Picotti 2006; Ba et al. 2008a,b, 2011). With the assumption of linearity, the research performed in recent years has been focused on the frequency dependence of P- and S- wave velocities and respective attenuation factors, caused by patchy saturation, pore distribution and rock microstructure.

According to Biot's theory, an isotropic poroelastic medium has four independent static moduli (or 2nd-order elastic constants (2oEC)). Biot (1973) developed a semilinear mechanical description of porous media, based on seven elastic constants. Four of them characterize the linear behaviour and three characterize the non-linear behaviour. The theory was adapted to solid-fluid composites by Norris, Sinha and Kostek (1994). Biot (1972) used an eleven-constant elastic potential function for fluid-saturated porous media. Drumheller and Bedford (1980) used an Eulerian reference frame to derive non-linear equations for wave propagation in porous media, while Berryman and Thigpen (1985) used a Lagrangian reference frame.

Donskoy, Khashanah and Mckee (1997) derived non-linear acoustic wave equations for porous media and established a correlation between measurable effective non-linear parameters and structural parameters of a porous medium. Their theory is based on the semilinear approximation of Biot's poroelasticity theory. The assumption of semilinearity implies a linear relation between the volume change of the solid matrix and the effective stress. Therefore, a modified strain is used (see Equations (7) and (54) in Biot 1973) and the effective stress is included, so that the non-linear acoustoelasticity equations can be simplified and only three independent 3oEC are necessary. Following this theoretical approach, Dazel and Tournat (2010) considered the 1D case and derived the solutions for second harmonic Biot waves. The wave-velocity dispersion and dissipation are analysed in a half-space. Zaitsev, Kolpakov and Nazarov (1999a,b) analysed the propagation of low-frequency signals in dry and water-saturated river sand and showed that the behaviour of loose granular media can be non-linear.

Grinfeld and Norris (1996) derived equations for wave velocities in closed-pore jacketed tests (CPJT) and open-pore jacketed (OPJT) tests, to find the seven 3oEC of a poroelastic medium. In the former, the pore fluid mass is constant (Grinfeld and Norris 1996), which means that the porous medium is surrounded by an impervious closed deformable jacket, so that the pore fluid cannot flow out of the rock frame. On the other hand, in the OPJT (Biot and Willis 1957; Johnson 1986; Grinfeld and Norris 1996) the fluid pressure is constant, because there is a tube where the fluid can flow in and out of the medium under an applied confining stress. However, the solid and fluid finite strains are not considered in their work, so the 2oEC do not appear in the term multiplying the confining pressure in the expressions of the velocities (see equation (1) below). This means that there is no compatibility between their poro-acoustoelasticity theory and the classical acoustoelasticity theory.

In this work, we generalize Grinfeld and Norris (1996)'s approach by including solid and fluid finite strains. Then, we derive the wave-propagation equations by substituting the eleven-term strain-energy function and Biot's kinetic and dissipation energies into Lagrange equations. The velocities and dissipation factors of the P- and S-waves are obtained as a function of the 2oEC and 3oEC and confining stress in the cases of hydrostatic and uniaxial loading conditions. We discuss the limit of this theory to the classical acoustoelasticity theory. Examples for wave velocity and dissipation are given for the OPJT and CPJT, respectively. Finally, we perform ultrasonic P-wave velocity measurements corresponding to these tests, under hydrostatic loading and compare the theoretical and experimental results.

NON-LINEAR THEORY. WAVE EQUATION

Classical acoustoelasticity

The non-linear 3oEC theory has been developed to describe wave propagation and mechanical deformations in a solid material. The strain energy function of an isotropic solid depends on three independent 3oEC. The relations between wave velocities and confining stresses were derived by Murnaghan (1951), Green (1973), Hughes and Kelly (1953), and Pao, Sachse and Fukuoka (1984):

$$
\begin{aligned}
\rho v_{Ph}^2 &= \lambda + 2\mu - \bar{P}(7\lambda + 10\mu + 6l + 4m),\\
\rho v_{Sh}^2 &= \mu - \bar{P}(3\lambda + 6\mu + 3m - 0.5n),\\
\rho v_{Px}^2 &= \lambda + 2\mu - \bar{T}\left[\frac{\lambda+\mu}{\mu}(4\lambda + 10\mu + 4m) + \lambda + 2l\right],\\
\rho v_{Py}^2 &= \lambda + 2\mu - \bar{T}\left[2l - \frac{2\lambda}{\mu}(\lambda + 2\mu + m)\right],\\
\rho v_{Sx}^2 &= \mu - \bar{T}\left(4\lambda + 4\mu + m + \frac{\lambda n}{4\mu}\right),\\
\rho v_{Sy}^2 &= \mu - \bar{T}\left(\lambda + 2\mu + m + \frac{\lambda n}{4\mu}\right),\\
\rho v_{Sz}^2 &= \mu - \bar{T}\left(m - 2\lambda - \frac{\lambda+\mu}{2\mu}n\right),
\end{aligned}
\tag{1}
$$

where,

$$\bar{P} = \frac{P}{3\lambda + 2\mu}, \quad \bar{T} = \frac{T}{3\lambda + 2\mu}, \tag{2}$$

P is hydrostatic (compressive) stress, T is the compressive stress applied along one of the three axes, λ and μ are the 2oEC (the Lamé constants), l, m and n are the 3oEC and ρ is the density. The subscripts P and S denote P and S waves and the subscript h indicates hydrostatic loading. Moreover, the subscript x denotes the direction along uniaxial loading. y and z denote the two directions perpendicular to uniaxial loading. For S waves propagating in the y direction, the particles vibrate along loading. For S waves propagating in the z direction, the particles vibrate perpendicular to loading.

Strain-energy function in poroelastic media

If the fluid-saturated rock is loaded with a high confining stress, infinitesimal strains are insufficient to describe the solid and fluid microscale finite deformations. In this case, we use the Lagrangian strain tensor

$$\epsilon_{ij} = \frac{1}{2}(u_{j,i} + u_{i,j} + u_{k,i}u_{k,j}), \quad i, j, k = 1, 2, 3, \tag{3}$$

where u_i denotes the solid displacement in the x_i-direction, and the convention of summation over repeated indices is adopted. Moreover, $u_{i,j}$ indicates a partial derivative of u_i with respect to x_j. In the following, the notation $(x, y, z) = (x_1, x_2, x_3)$ is used.

Non-linear acoustics of fluids is usually formulated in terms of an Eulerian description of wave motion (Beyer 1960, 1984). Kostek, Sinha and Norris (1993) provided explicit relations for the Lagrangian and Eulerian descriptions of an inviscid fluid. In non-linear problems involving fluids and solids, the unified treatment of Lagrangian variables is used. If we neglect the fluid shear deformations, the fluid finite strain can be approximately written as

$$\theta_{i(i)} = U_{(i),i} + \frac{1}{2}U^2_{(i),i}, \tag{4}$$

where U_i denotes the fluid displacement in the x_i-direction. This approximation can be applied to light fluids, such as water, oil and gas. For non-Newtonian media, such as bitumen and heavy oil, shear deformations have to be considered.

In an isotropic medium, the strain energy can be expressed as

$$\begin{aligned} 2W = {} & M_1 I_1^2 + M_2 I_2 + M_3\theta^2 + M_4\theta I_1 + M_5 I_1^3 + M_6 I_3 \\ & + M_7\theta^3 + M_8 I_1 I_2 + M_9\theta I_2 + M_{10} I_1^2\theta + M_{11} I_1\theta^2, \end{aligned} \tag{5}$$

where M_l, $l = 1, \ldots, 11$ are the elasticity constants,

$$\epsilon = u_{i,i} \quad \text{and} \quad \theta = U_{i,i}. \tag{6}$$

The invariants are

$$\begin{aligned} I_1 &= \epsilon = \epsilon_{11} + \epsilon_{22} + \epsilon_{33}, \\ I_2 &= \begin{vmatrix} \epsilon_{11} & \epsilon_{12} \\ \epsilon_{12} & \epsilon_{22} \end{vmatrix} + \begin{vmatrix} \epsilon_{11} & \epsilon_{13} \\ \epsilon_{13} & \epsilon_{33} \end{vmatrix} + \begin{vmatrix} \epsilon_{22} & \epsilon_{23} \\ \epsilon_{23} & \epsilon_{33} \end{vmatrix}, \\ I_3 &= \begin{vmatrix} \epsilon_{11} & \epsilon_{12} & \epsilon_{13} \\ \epsilon_{12} & \epsilon_{22} & \epsilon_{23} \\ \epsilon_{13} & \epsilon_{23} & \epsilon_{33} \end{vmatrix}. \end{aligned} \tag{7}$$

Expression (5) is similar to that of Biot (1972) (his equation (5.9)), but the variation of fluid content has been replaced by θ, therefore, the elastic constants are not the same. The strain energy depends on four 2oEC ($M_1, \ldots, M_4$) and seven 3oEC ($M_5, \ldots, M_{11}$).

The solid and fluid stress components are given by

$$\sigma_{ij} = \frac{\partial W}{\partial \epsilon_{ij}} \quad \text{and} \quad \tau_{ij} = \frac{\partial W}{\partial \theta_{ij}}, \quad i, j = 1, 2, 3, \tag{8}$$

The 2oEC are those obtained by Biot and Willis (1957) by means of 'gedanken' experiments (e.g., Carcione 2007)

$$\begin{aligned} M_1 &= P = K_m + M(\gamma - \phi)^2 + \frac{4}{3}\mu_m, \\ M_2 &= -4N = -4\mu_m, \\ M_3 &= R = M\phi^2, \\ M_4 &= 2Q = 2M\phi(\gamma - \phi), \end{aligned} \tag{9}$$

where

$$M = \frac{K_s}{1 - \phi - K_m/K_s + \phi K_s/K_f}, \tag{10}$$

$$\gamma = 1 - \frac{K_m}{K_s}, \tag{11}$$

with K_m, K_s and K_f the bulk moduli of the drained matrix, solid and fluid, respectively; ϕ is the porosity and μ_m is the shear modulus of the drained as well as saturated matrix. The notations P, A, N, R and Q are as in Biot (1956) (do not confuse this P with the hydrostatic stress introduced in equation (2)).

On the other hand, in the limit to the classical acoustoelasticity theory, the equivalences are

$$\begin{aligned} &M_1 + M_3 + M_4 = \lambda + 2\mu, \\ &M_2 = -4\mu, \\ &M_6 = 2n, \\ &M_5 + M_7 + M_{10} + M_{11} = \frac{2}{3}(l + 2m), \\ &M_8 + M_9 = -4m. \end{aligned} \tag{12}$$

The determination of the seven 3oEC requires additional 'gedanken' experiments, which will be the subject of future work.

Kinetic and dissipation energies

In this work, we use a theoretical approach similar to those of Biot (1962) and Norris (1996) but finite strain is used instead of infinitesimal strain. The dissipation function and the kinetic energy per unit volume of isotropic fluid-solid composite are given by (Biot 1962)

$$2D = \frac{\phi^2 \eta}{\kappa}[(\dot{u}_1 - \dot{U}_1)^2 + (\dot{u}_2 - \dot{U}_2)^2 + (\dot{u}_3 - \dot{U}_3)^2] \tag{13}$$

and

$$\begin{aligned} 2T = {} & \rho_{11}(\dot{u}_1^2 + \dot{u}_2^2 + \dot{u}_3^2) + 2\rho_{12}(\dot{u}_1\dot{U}_1 + \dot{u}_2\dot{U}_2 + \dot{u}_3\dot{U}_3) \\ & + \rho_{22}\left(\dot{U}_1^2 + \dot{U}_2^2 + \dot{U}_3^2\right), \end{aligned} \tag{14}$$

respectively, where

$$\begin{aligned} &\rho_{11} = (1 - \phi)\rho_s - \rho_{12}, \\ &\rho_{22} = \phi\rho_f - \rho_{12}, \\ &\rho_{12} = -\phi\rho_f(\mathcal{T} - 1), \end{aligned}$$

where ρ_s and ρ_f are the solid and fluid mass densities and $\mathcal{T}$ is the tortuosity (Biot 1956; Carcione 2007), η is the fluid viscosity, κ is the permeability and a dot above a variable denotes time differentiation.

Lagrange and wave equations

Applying Lagrange's equations and taking u_i and U_i as generalized coordinates, the generalized forces corresponding to the solid and fluid phases can be expressed as

$$\begin{aligned} f_i &= \frac{d}{dt}\left(\frac{\partial T}{\partial \dot{u}_i}\right) + \frac{\partial D}{\partial \dot{u}_i}, \\ F_i &= \frac{d}{dt}\left(\frac{\partial T}{\partial \dot{U}_i}\right) + \frac{\partial D}{\partial \dot{U}_i}, \end{aligned} \tag{15}$$

where

$$f_i = \frac{d}{dx_j}\frac{\partial W}{\partial u_{i,j}}, \quad F_i = \frac{d}{dx_j}\frac{\partial W}{\partial U_{i,j}}.$$

Let us define

$$\begin{aligned} \mathbf{J} &= \begin{pmatrix} 1 + u_{1,1} & u_{1,2} & u_{1,3} \\ u_{2,1} & 1 + u_{2,2} & u_{2,3} \\ u_{3,1} & u_{3,2} & 1 + u_{3,3} \end{pmatrix} \quad \text{and} \\ \mathbf{K} &= \begin{pmatrix} 1 + U_{1,1} & 0 & 0 \\ 0 & 1 + U_{2,2} & 0 \\ 0 & 0 & 1 + U_{3,3} \end{pmatrix}. \end{aligned} \tag{16}$$

Using equations (8)–(16), we obtain the non-linear wave equations of the two-phase medium,

$$\begin{aligned} &\sigma_{ik,j}\mathbf{J}_{kj} + \sigma_{ik}\mathbf{J}_{kj,j} = \rho_{11}\ddot{u}_i + \rho_{12}\ddot{U}_i + b(\dot{u}_i - \dot{U}_i), \\ &\tau_{ik,j}\mathbf{K}_{kj} + \tau_{ik}\mathbf{K}_{kj,j} = \rho_{12}\ddot{u}_i + \rho_{22}\ddot{U}_i - b(\dot{u}_i - \dot{U}_i), \end{aligned} \tag{17}$$

where $b = \phi^2\eta/k$.

NON-LINEAR THEORY. DISPERSION EQUATIONS

The complex velocity of a given wave mode is given by

$$v = \frac{\omega}{k}, \tag{18}$$

where ω is the angular frequency and k is the complex and frequency dependent wavenumber. The phase velocity and dissipation factor are

$$v_p = \left[\mathrm{Re}\left(\frac{1}{v}\right)\right]^{-1} \quad \text{and} \quad \frac{1}{Q} = \frac{\mathrm{Im}(v^2)}{\mathrm{Re}(v^2)} \tag{19}$$

respectively, where 'Re' and 'Im' take real and imaginary parts (e.g., Carcione 2007). The dissipation factor is the reciprocal of the quality factor Q.

In the following, we obtain the dispersion equations for hydrostatic and uniaxial loadings, which give the complex and frequency-dependent wavenumbers and corresponding velocities as a function of the loading stress.

Hydrostatic confining stress

For simplicity, let us consider a plane P-wave propagating in the x-direction. Wave equations (17) become

$$\begin{aligned} &\sigma_{11,1} + \sigma_{11,1}u_{1,1} + \sigma_{11}u_{1,11} = \rho_{11}\ddot{u}_1 + \rho_{12}\ddot{U}_1 + b(\dot{u}_1 - \dot{U}_1), \\ &\tau_{11,1} + \tau_{11,1}U_{1,1} + \tau_{11}U_{1,11} = \rho_{12}\ddot{u}_1 + \rho_{22}\ddot{U}_1 - b(\dot{u}_1 - \dot{U}_1). \end{aligned} \tag{20}$$

The total strains applied to the solid and fluid phases are

$$\boldsymbol{\epsilon} = \boldsymbol{\epsilon}_1 + \boldsymbol{\epsilon}_2 \quad \text{and} \quad \boldsymbol{\theta} = \boldsymbol{\theta}_1 + \boldsymbol{\theta}_2,$$

where the subscripts '1' and '2' indicate the contributions of the large strain induced by the hydrostatic static loading and that of the propagating wave, respectively.

For a hydrostatic loading, we have

$$\boldsymbol{\epsilon}_1 = \begin{pmatrix} \alpha & 0 & 0 \\ 0 & \alpha & 0 \\ 0 & 0 & \alpha \end{pmatrix} \quad \text{and} \quad \boldsymbol{\theta}_1 = \begin{pmatrix} \beta & 0 & 0 \\ 0 & \beta & 0 \\ 0 & 0 & \beta \end{pmatrix}. \tag{21}$$

The contribution of the small strain induced by the P waves is

$$\begin{aligned} \boldsymbol{\epsilon}_2 &= \begin{pmatrix} 1 & 0 & 0 \\ 0 & 0 & 0 \\ 0 & 0 & 0 \end{pmatrix} \epsilon_0 \exp[\omega t - kx(1+\alpha)] \quad \text{and} \\ \boldsymbol{\theta}_2 &= \begin{pmatrix} 1 & 0 & 0 \\ 0 & 0 & 0 \\ 0 & 0 & 0 \end{pmatrix} \theta_0 \exp[\omega t - kx(1+\beta)], \end{aligned} \tag{22}$$

where ϵ_0 and θ_0 are wave amplitudes. Substituting equations (21) and (22) into equations (20), neglecting terms whose power is higher than 1 and eliminating ϵ_0 and θ_0, yields the following dispersion equation,

$$\begin{vmatrix} \Upsilon_1 k^2 - \rho_{11}\omega^2 + \mathrm{i}b\omega & (\Upsilon_2 + M_4\beta)k^2 - \rho_{12}\omega^2 - \mathrm{i}b\omega \\ (\Upsilon_2 + M_4\alpha)k^2 - \rho_{12}\omega^2 - \mathrm{i}b\omega & \Upsilon_3 k^2 - \rho_{22}\omega^2 + \mathrm{i}b\omega \end{vmatrix} = 0, \tag{23}$$

where $\mathrm{i} = \sqrt{-1}$,

$$\Upsilon_1 = M_1 + (7M_1 + M_2 + 9M_5 + 2M_8)\alpha + \left(\frac{3}{2}M_4 + 3M_{10}\right)\beta,$$

$$\Upsilon_2 = \frac{1}{2}M_4 + \left(\frac{1}{2}M_4 + M_9 + 3M_{10}\right)\alpha + \left(\frac{1}{2}M_4 + 3M_{11}\right)\beta,$$

$$\Upsilon_3 = M_3 + \left(\frac{3}{2}M_4 + 3M_{11}\right)\alpha + (9M_7 + 7M_3)\beta.$$

The complex and frequency dependent fast and slow P-wave velocities correspond to two solutions of the quadratic equation (23).

Similarly to the low-frequency limit of Biot equations, which yields Gassmann equations (Gassmann 1951), neglecting the relative motion between the solid and fluid phases, equation (23) gives

$$\rho v^2 = \Upsilon_1 + 2\Upsilon_2 + \Upsilon_3 + M_4(\alpha + \beta), \tag{24}$$

where $\rho = \rho_{11} + 2\rho_{12} + \rho_{22}$ is the bulk density (Biot 1962). Expression (24) is a non-linear generalization of the Gassmann equation. If $\alpha = \beta$ (solid and fluid finite strains are the same), we obtain

$$\begin{aligned} \rho v^2 = {} & M_1 + M_3 + M_4 + [7(M_1 + M_3 + M_4) + M_2 \\ & + 9(M_5 + M_7 + M_{10} + M_{11}) + 2(M_8 + M_9)]\alpha. \end{aligned} \tag{25}$$

Using equivalences (12), equation (25) is identical to the first equation in (1) if $\alpha = -\bar{P}$.

For plane S-waves propagating along the y-direction, with polarization in the x-direction, we have

$$\begin{aligned} &\sigma_{12,2} + \sigma_{12,2}u_{1,1} + \sigma_{22}u_{1,22} = \rho_{11}\ddot{u}_1 + \rho_{12}\ddot{U}_1 + b(\dot{u}_i - \dot{U}_1), \\ &0 = \rho_{12}\ddot{u}_i + \rho_{22}\ddot{U}_1 - b(\dot{u}_1 - \dot{U}_1). \end{aligned} \tag{26}$$

The infinitesimal dynamic strain induced by the S-waves has the form of equation (22), replacing x by y. The dispersion equation is

$$\begin{vmatrix} \Psi k^2 - \rho_{11}\omega^2 + \mathrm{i}b\omega & -\rho_{12}\omega^2 - \mathrm{i}b\omega \\ -\rho_{12}\omega^2 - \mathrm{i}b\omega & -\rho_{22}\omega^2 + \mathrm{i}b\omega \end{vmatrix} = 0, \tag{27}$$

where

$$\Psi = -\frac{M_2}{4} + \left(3M_1 - \frac{M_6}{4} - \frac{3}{4}M_8\right)\alpha + \left(\frac{3}{2}M_4 - \frac{3}{4}M_9\right)\beta.$$

The frequency-dependent S-wave velocity can be obtained from (27).

To obtain the acoustoelasticty limit, let us assume that the pore fluid suffers the same static deformation of the frame. Equation (27) becomes

$$\rho v^2 = -\frac{M_2}{4} + \left(3M_1 + \frac{3}{2}M_4 - \frac{M_6}{4} - \frac{3}{4}M_8 - \frac{3}{4}M_9\right)\alpha. \tag{28}$$

This equation is not the second equation in (1), since fluid shear effects were neglected in equation (26). If these terms are not neglected, the left-hand side of the second equation in (26) becomes $\tau_{12,2} + \tau_{12,2}U_{1,1} + \tau_{22}U_{1,22}$, which gives two additional terms $3M_4\alpha/2$ and $3M_3\beta$.

We obtain the second equation in (1) by neglecting the solid-fluid relative deformation and adding the fluid shear terms, i.e.,

$$\rho v^2 = -\frac{M_2}{4} + \left(3M_1 + 3M_4 + 3M_3 - \frac{M_6}{4} - \frac{3}{4}M_8 - \frac{3}{4}M_9\right)\alpha. \tag{29}$$

Uniaxial confining stress

For an uniaxial loading T in the x-direction, the large (finite) static strains, induced by the confining stress, have the form of equation (21), replacing α by $\alpha' \neq \alpha$ in the (22) and (33) elements of matrix $\boldsymbol{\epsilon}_1$. The dynamic strain, induced by a plane P-wave, with polarization in the x-direction, has the form of

equation (22). Then, the dispersion equation has the form of equation (23), where

$$\Upsilon_1 = M_1 + (5M_1 + 3M_5)\alpha + (2M_1 + M_2 + 6M_5 + 2M_8)\alpha' + \left(\frac{3}{2}M_4 + 3M_{10}\right)\beta,$$

$$\Upsilon_2 = \frac{1}{2}M_4 + \left(\frac{1}{2}M_4 + M_{10}\right)\alpha + (M_9 + 2M_{10})\alpha' + \left(\frac{1}{2}M_4 + 3M_{11}\right)\beta,$$

$$\Upsilon_3 = M_3 + \left(\frac{1}{2}M_4 + M_{11}\right)\alpha + (M_4 + 2M_{11})\alpha' + (9M_7 + 7M_3)\beta.$$

If the differential motion between the solid and the fluid is neglected, we have

$$\rho v^2 = \Upsilon_1 + 2\Upsilon_2 + \Upsilon_3 + M_4(\alpha + \beta). \tag{30}$$

Equation (30) can be directly reduced to the third equation in (1) if we replace β by α along the x-direction and β by α' along the perpendicular directions, i.e.,

$$\begin{aligned}\rho v^2 = {} & M_1 + M_3 + M_4 + [5(M_1 + M_3 + M_4) \\ & + 3(M_5 + M_7 + M_{10} + M_{11})]\alpha \\ & + [2(M_1 + M_3 + M_4) + M_2 \\ & + 6(M_5 + M_7 + M_{10} + M_{11}) + 2(M_8 + M_9)]\alpha',\end{aligned} \tag{31}$$

where

$$\alpha = -\frac{(\lambda + \mu)T}{\mu(3\lambda + 2\mu)} \quad \text{and} \quad \alpha' = \frac{\lambda T}{2\mu(3\lambda + 2\mu)}.$$

On the other hand, for S waves travelling along the direction perpendicular to the loading with polarization along the loading direction, the infinitesimal dynamic strain has the form of equation (22), replacing x by y and the dispersion equation has the form of equation (27), with

$$\Psi = -\frac{M_2}{4} + \left(3M_1 - \frac{1}{4}M_8\right)\alpha + \left(2M_1 - \frac{1}{2}M_8 - \frac{1}{4}M_6\right)\alpha' + \left(\frac{3}{2}M_4 - \frac{3}{4}M_9\right)\beta.$$

Replacing β with α and α' in different directions and including the fluid shear terms, the solution reduces to the sixth equation in (1),

$$\begin{aligned}\rho v^2 = {} & -\frac{M_2}{4} + [(M_1 + M_3 + M_4)(\alpha + 2\alpha') - \frac{M_6}{4}\alpha' \\ & - \frac{1}{4}(M_8 + M_9)(\alpha + 2\alpha')].\end{aligned} \tag{32}$$

For P waves propagating along the x-direction and uniaxial-loading along the y-direction, the large strains induced by the load have the form of equation (21), replacing α by $\alpha' \neq \alpha$ in the (11) and (33) elements of matrix $\boldsymbol{\epsilon}_1$. The infinitesimal strains have the form of equation (22), replacing α by α' in the exponent of the first expression. Therefore, the dispersion equation has the form of equation (22), replacing α by α' in the (21) element inside the determinant with

$$\Upsilon_1 = M_1 + \left(M_1 + \frac{1}{2}M_2 + 3M_5 + M_8\right)\alpha + \left(6M_1 + \frac{1}{2}M_2 + 6M_5 + M_8\right)\alpha' + \left(\frac{3}{2}M_4 + 3M_{10}\right)\beta,$$

$$\Upsilon_2 = \frac{1}{2}M_4 + \left(\frac{1}{2}M_9 + M_{10}\right)\alpha + \left(\frac{1}{2}M_4 + \frac{1}{2}M_9 + 2M_{10}\right)\alpha' + \left(\frac{1}{2}M_4 + 3M_{11}\right)\beta,$$

$$\Upsilon_3 = M_3 + \left(\frac{1}{2}M_4 + M_{11}\right)\alpha + (M_4 + 2M_{11})\alpha' + (9M_7 + 7M_3)\beta.$$

The solution becomes the fourth equation in (1) if the relative fluid-solid motion is neglected and $\beta = \alpha$,

$$\begin{aligned}\rho v^2 = {} & M_1 + M_3 + M_4 + [M_1 + M_3 + M_4 + \frac{M_2}{2} \\ & + 3(M_5 + M_7 + M_{10} + M_{11}) + M_8 + M_9]\alpha \\ & + [6(M_1 + M_3 + M_4) + \frac{1}{2}M_2 \\ & + 6(M_5 + M_7 + M_{10} + M_{11}) + M_8 + M_9]\alpha'.\end{aligned} \tag{33}$$

For S waves propagating along the uniaxial-loading direction, the static strains have the form of equation (21), replacing α by $\alpha' \neq \alpha$ in the (11) and (33) elements of matrix $\boldsymbol{\epsilon}_1$, and the dynamic strain has the form of equation (22), replacing x by y. Then, the dispersion equation has the form of equation (27), with

$$\Psi = -\frac{M_2}{4} + \left(M_1 - \frac{M_2}{2} - \frac{M_8}{4}\right)\alpha + \left(2M_1 + \frac{M_2}{2} - \frac{M_8}{2} - \frac{M_6}{4}\right)\alpha' + \left(\frac{3}{2}M_4 - \frac{3}{4}M_9\right)\beta.$$

The fifth equation in (1) can be obtained from this expression as a particular case,

$$\begin{aligned}\rho v^2 = {} & -\frac{M_2}{4} + [(M_1 + M_3 + M_4)(\alpha + 2\alpha') - \frac{M_2}{2}(\alpha - \alpha') \\ & - \frac{M_6}{4}\alpha' - \frac{1}{4}(M_8 + M_9)(\alpha + 2\alpha')].\end{aligned} \tag{34}$$

Table 1 Properties of the sandstone.

M_1	8.56	ρ_s	2650 kg/m^3
M_2	−11.7	ρ_f	1040 kg/m^3
M_3	0.75	$\mathcal{T}$	2
M_4	2.7	ϕ	0.335
M_5	244	κ	1 D
M_6	131	η	0.0015 Pa s
M_7	7	K_s	36.7 GPa
M_8	−450	K_f	2.51 GPa
M_9	−150	K_m	2.23 GPa
M_{10}	65	μ_m	2.93 GPa
M_{11}	24		

The elasticity constants are given in GPa.

Finally, for S waves propagating along the direction perpendicular to the uniaxial-loading direction, whose polarization is also perpendicular to this direction, the dynamic strain has the form of equation (22), replacing x by z in both expressions and α by α' in the exponent of the first expression. Then, the dispersion equation has the form of equation (27), with

$$\Psi = -\frac{M_2}{4} + \left(M_1 + \frac{M_2}{2} - \frac{M_8}{4} - \frac{M_6}{4}\right)\alpha + \left(2M_1 - \frac{1}{2}M_2 - \frac{M_8}{2}\right)\alpha' + \left(\frac{3}{2}M_4 - \frac{3}{4}M_9\right)\beta.$$

The dispersion equation yields the seventh equation in (1) as a particular case,

$$\rho v^2 = -\frac{M_2}{4} + [(M_1 + M_3 + M_4)(\alpha + 2\alpha') + \frac{M_2}{2}(\alpha - \alpha') - \frac{M_6}{4}\alpha' - \frac{1}{4}(M_8 + M_9)(\alpha + 2\alpha')]. \quad (35)$$

Dispersion equations (23) and (27) are the main results of this work.

RESULTS

The elasticity and density coefficients of a water-saturated rock are given in Table 1. The 2oEC and density coefficients are taken from Dai, Vafidis and Kanasewich (1995), while the seven 3oEC are assumed (we assume the ratio between 3oEC and 2oEC is consistent with the acoustoelasticity theory of a pure solid, while the ratio between two different 3oECs is close to the ratio between two different 2oECs in Biot's theory).

Wave velocities for hydrostatic loading

In the OPJT (Fig. 1b in Grinfeld and Norris 1996) and a hydrostatic stress P acting on the frame, Biot's stress-strain relations are $P = (A + 2N/3)\epsilon + Q\theta$ and $0 = Q\epsilon + R\theta$ (e.g., Carcione 2007). Substituting $\alpha = \epsilon/3$ and $\beta = \theta/3$ into equations (23) and (27) yields the OPJT velocities. On the other hand, in the CPJT (Fig. 1a in Grinfeld and Norris 1996), the relations are $P_s = (A + 2N/3)\epsilon + Q\theta$ and $P_f = Q\epsilon + R\theta$, where $P = P_s + P_f$ and $P_f/\phi = K_f\theta$. Solving for the solid and fluid strains ϵ and θ and substituting them into equations (23) and (27) yield the CPJT velocities.

Figures 1 and 2 show the velocities and dissipation factors corresponding to the two experiments as a function of the confining pressure P. As can be seen, the fast P-wave dissipation factor and the S-wave velocity are sensitive to the change in hydrostatic pressure. The fast P-wave attenuation significantly increases in the loading process, with higher values in the open-pore case. The (11)-component in equation (23) is the most significant term and yields higher Biot loss in the OPJT, since Υ_1 is higher in this case. This difference increases with increasing load. The slow P-wave velocity has a maximum at 13 MPa in the OPJT. Moreover, the S-wave attenuation is not affected by hydrostatic stress and the slow P-wave attenuation has a negligible variation, so these curves are not shown.

The CPJT has lower fast P-wave velocities and higher S- and slow P-wave velocities. The fast P-wave dissipation factor is lower than that predicted for the OPJT. In any case, the dissipation is low, agreeing with the classical Biot values. In the OPJT, the loading acts on the frame and its non-linear features dominate. In the CPJT, the fluid pressure compensates the external stress and the bulk is effectively less compressed, implying a lower velocity. Figure 2 shows that velocity and attenuation are more sensitive to stress than frequency (the opposite occurs for the slow wave). The S-wave attenuation shows no changes with loading. The fast P-wave velocity of the OPJT is much higher than the corresponding velocity of the CPJT as loading increases, while the OPJT dissipation factor is lower than the CPJT dissipation factor for stresses below 5 MPa, but becomes much higher beyond 30 MPa.

Pores are assumed to be equant (stiff) as in Biot (1962) and therefore local fluid-flow effects are not considered in this work. Attenuation due to this phenomenon can be one or two orders of magnitude higher than that generated by Biot's global flow (e.g., Ba et al. 2008b; Ba, Carcione and Nie 2011).

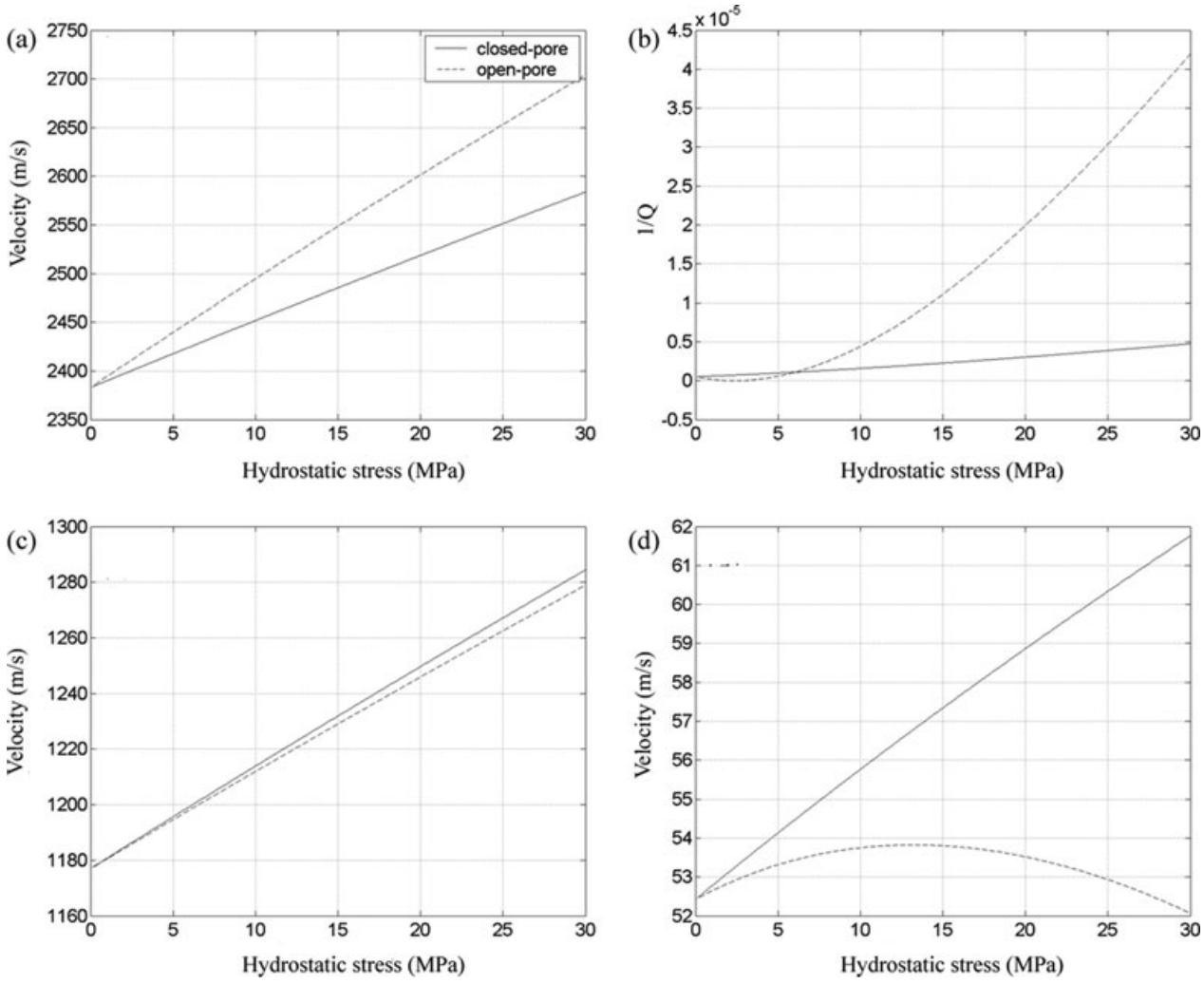

Figure 1 Velocities and dissipation factor versus hydrostatic stress at 1 MHz. (a) and (b): fast P wave; (c): S wave; (d) slow P wave. The solid and dashed lines correspond to the closed-pore and open-pore jacketed tests, respectively.

Wave velocities for uniaxial loading

First, we consider the open-pore jacketed test. Biot's stress-strain relation under an uniaxial load T are $T = A\epsilon + 2N\epsilon_{11} + Q\theta$, $0 = A\epsilon + 2N\epsilon_{22} + Q\theta$ and $0 = Q\epsilon + R\theta$. Since $\epsilon = \epsilon_{11} + 2\epsilon_{22}$, ϵ_{11}, ϵ_{22} and θ can be obtained. Substituting $\alpha = \epsilon_{11}$, $\alpha' = \epsilon_{22}$ and $\beta = \theta/3$ into equations (23) and (27), we obtain the velocities and dissipation factors.

Figure 3 shows the velocities and dissipation factors as a function of the uniaxial loading T. The fast P-wave velocity changes more in the loading direction than along the perpendicular direction, since microcracks in the loading direction are more sensitive. The slow P-wave velocity slightly increases in the perpendicular direction and slightly decreases in the parallel direction. For the same loading value, the fast P-wave attenuation is higher in the parallel direction if the load exceeds 5 MPa but the loss is lower than in the previous tests. These results are consistent with the predictions of the classical acoustoelasticity theory. The S-wave velocities along the loading direction are higher and the S wave, whose polarization is parallel to the loading direction, has the lower velocities. All three S-wave velocities are lower than those of the OPJT.

The results shown in Fig. 1(b) and Fig. 3(b) predict that attenuation increases with loading, which is not in agreement with experimental data (Guo, Fu and Ba 2009). This is because local fluid flow effects are not considered.

Let us consider now, the closed-pore jacketed test. In this case, the stress-strain relations are $T_1 = A\epsilon + 2N\epsilon_{11} + Q\theta$, $T_2 = A\epsilon + 2N\epsilon_{22} + Q\theta$, $T_f = Q\epsilon + R\theta$, $T = T_1 + T_f$, $0 = T_2 + T_f$ and $T_f/\phi = K_f\theta$, where T_1 and T_2 are the stress

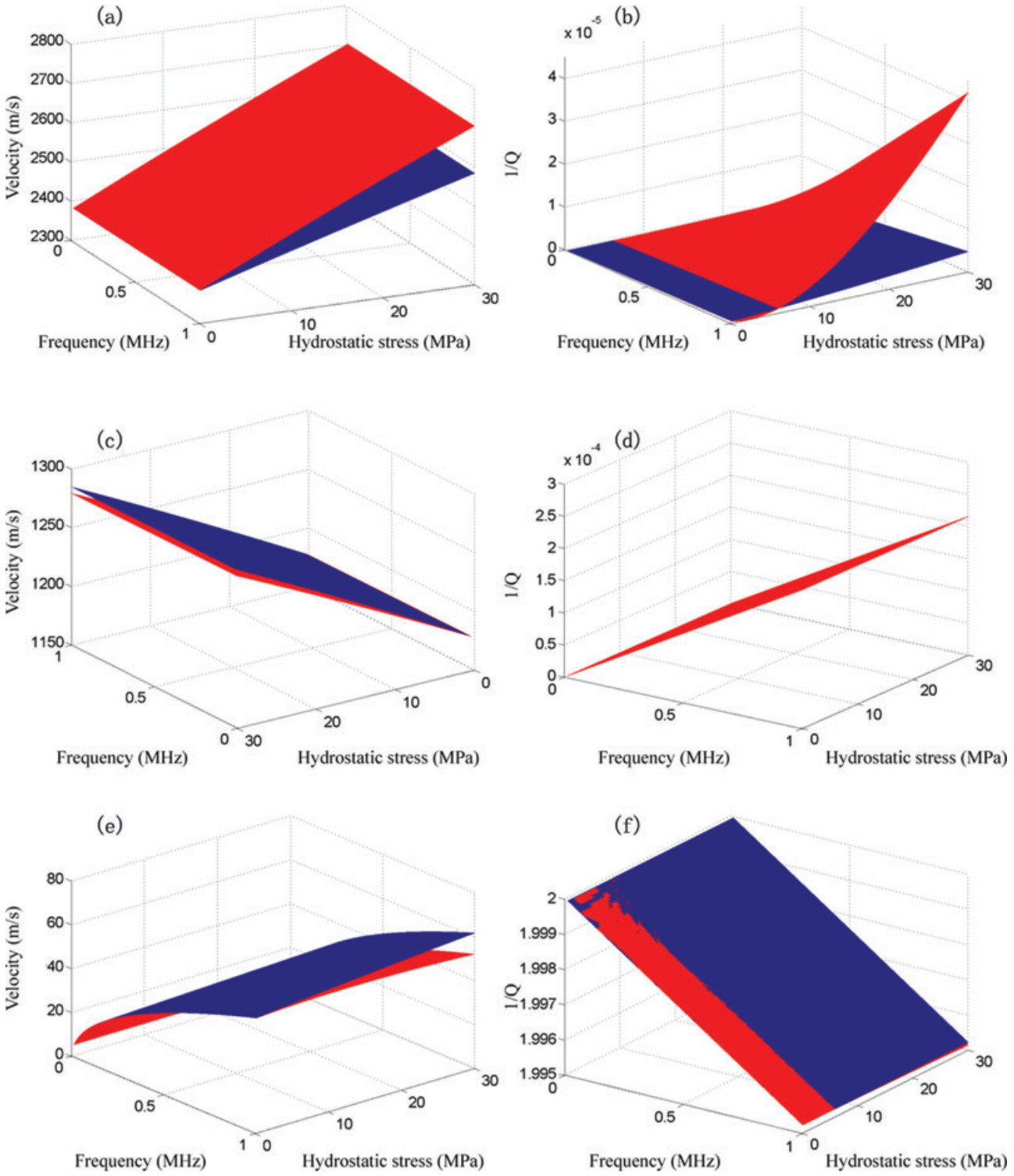

Figure 2 Velocities and dissipation factor as a function of stress and frequency. (a) and (b): fast P wave; (c) and (d): S wave; (e) and (f): slow P wave. Blue and red correspond to the closed-pore and open-pore jacketed tests, respectively.

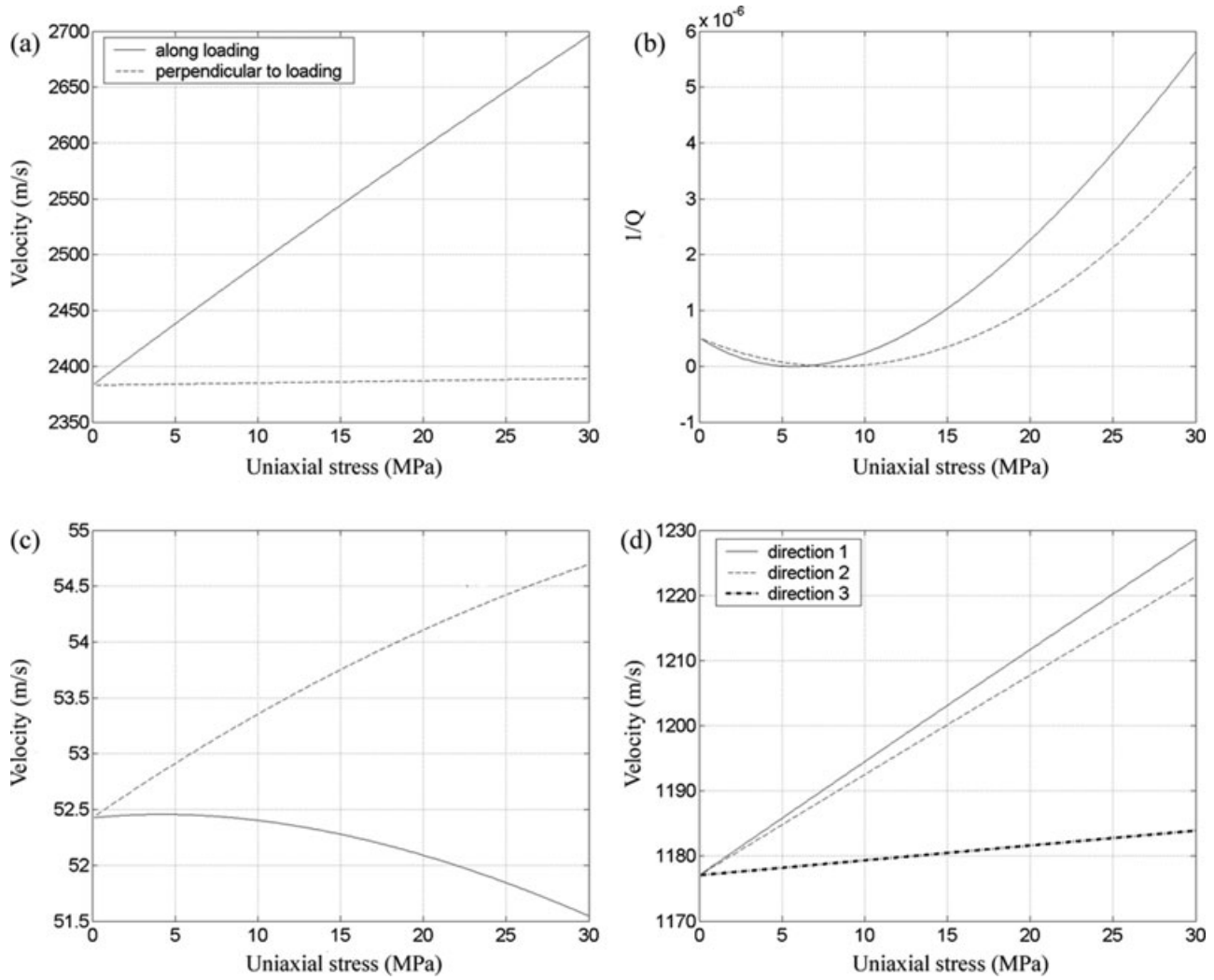

Figure 3 Velocities and dissipation factor as a function of uniaxial load at 1 MHz for the open-pore jacketed test. (a) and (b): fast P wave; (c): slow P wave; (d) S wave. In (a)-(c), the solid and dashed lines correspond to the directions perpendicular and along to the loading direction, respectively. In (d), '1' denotes a wave propagating along the loading direction with normal polarization, '2' denotes a wave propagating perpendicular to the loading direction with parallel polarization, and '3' denotes a wave propagating perpendicular to the loading direction with normal polarization.

acting on the solid along and perpendicular to the loading direction, respectively.

Figure 4 shows the velocities and dissipation factors as a function of the uniaxial loading T. Contrary to the previous trends, the fast P-wave velocity perpendicular to the loading direction decreases (slightly) with increasing load, while the corresponding velocity increases along this direction. The fast P-wave dissipation factor perpendicular to loading increases with loading. The trend of the S-wave velocity is to increase with T, with the highest values in the loading direction.

COMPARISON TO EXPERIMENTAL DATA

The two hydrostatic loading tests, OPJT and CPJT, were performed on sandstone having a porosity $\phi = 0.13$ and a permeability $\kappa = 1.21$ mD. The sample comes from a gas reservoir located at approximately 2 km depth in south-west China. The sample is mainly composed of quartz and feldspar, with clay partially filling the pores. The grain size ranges from 0.1–1 mm, while the pores have a maximum size of 0.4 mm. The average grain density is 2659 kg/cm^3 and the grain bulk modulus is 39 GPa.

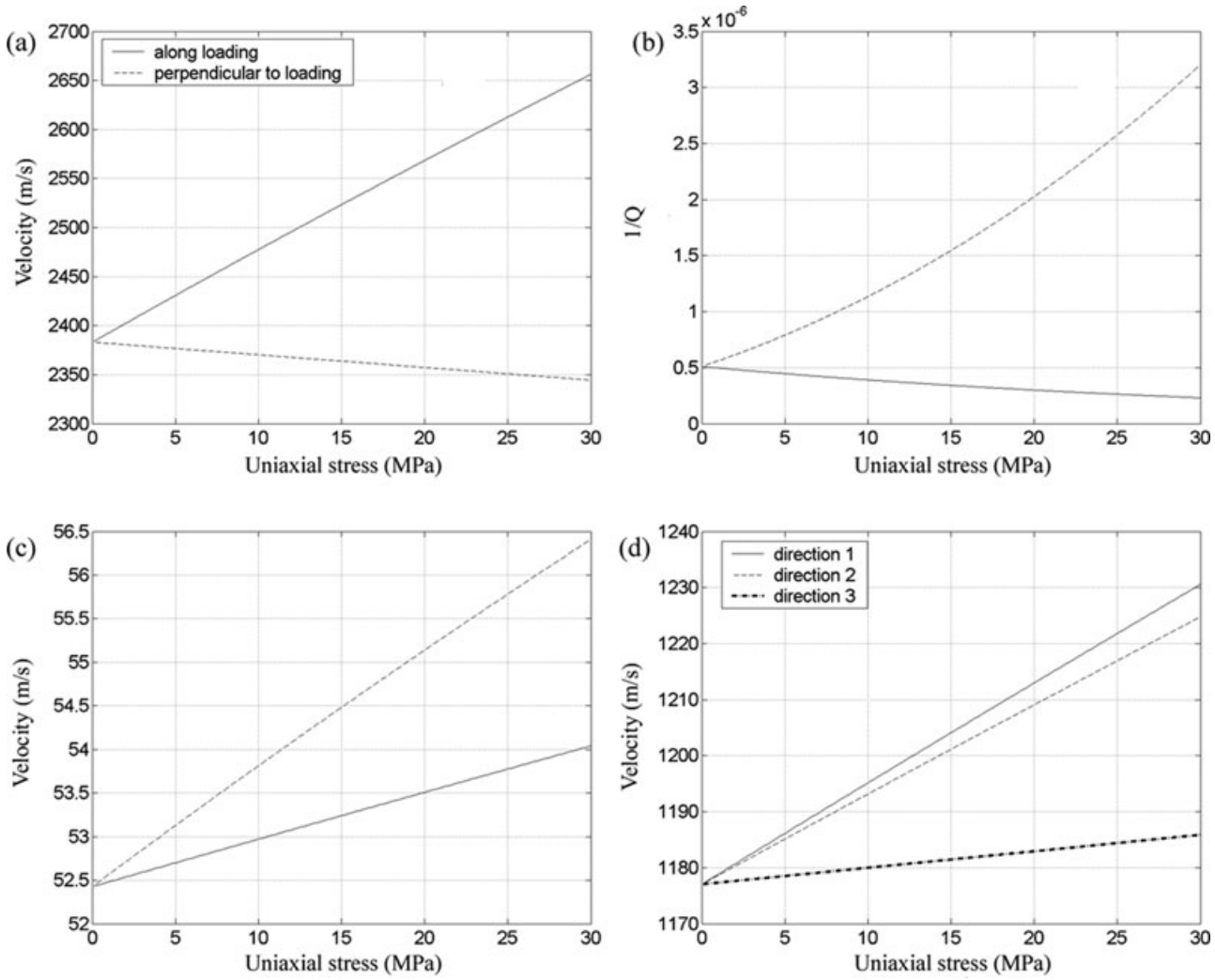

Figure 4 Velocities and dissipation factor as a function of uniaxial load at 1 MHz for the closed-pore jacketed test. (a) and (b): fast P wave; (c): slow P wave; (d) S wave. In (a)-(c), the solid and dashed lines correspond to the directions perpendicular to and along the loading direction, respectively. In (d), '1' denotes a wave propagating along the loading direction with normal polarization, '2' denotes a wave propagating perpendicular to the loading direction with parallel polarization, and '3' denotes a wave propagating perpendicular to the loading direction with normal polarization.

The experimental setup consists in a digital oscilloscope and a pulse generator. In the test, the rock sample is jacketed with a rubber. The receiving transducer is connected to the digitizing board in a PC through a signal amplifier. A pore fluid inlet in the endplate allows the passage of pore fluid through the sample and allows us to control the pore pressure. We performed a small modification on the original inlet instrument by adding a valve (it is closely connected to the inlet), so that the CPJT can be realized. In each test, the rock is fully saturated with water and both confining stress and pore pressure are increased to 30 MPa. In the CPJT, we close the valve and increase the confining stress from 10–62 MPa with steps of 4 MPa. In the OPJT, the valve is open. The pore pressure is close to the atmospheric pressure, when the confining stress is not high (it can be neglected compared to the confining load).

On the basis of the poro-acoustoelasticity theory, eleven elasticity constants have to be determined to predict the velocity-stress relationship. The four 2oEC can be obtained from the Biot-Gassmann theory (Johnson, 1986; Carcione 2007). The dry-rock bulk modulus can be estimated from the relation $K_m = K_s(1 - \phi)/(1 + c\phi)$, where c is the consolidation parameter (Pride et al. 2004). We take $c = 8$ since the porosity is not so high and the rock is consolidated. The four 2oEC are $M_1 = 37.4$ GPa, $M_2 = -53.6$ GPa, $M_3 = 0.273$

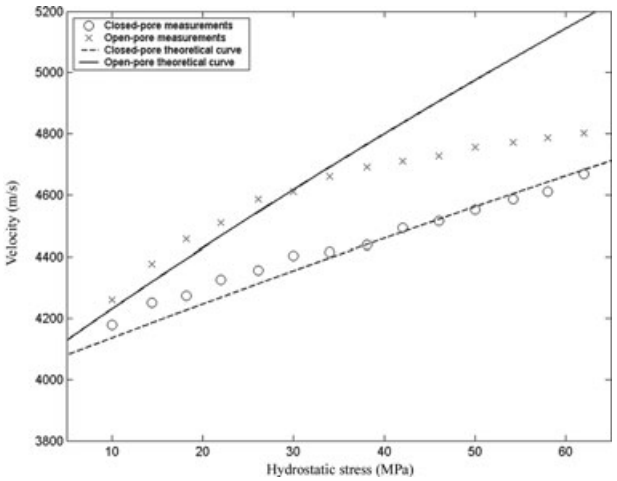

Figure 5 Comparison between the experimental and theoretical P-wave velocities, corresponding to the open-pore and closed-pore jacketed tests.

GPa and $M_4 = 1.84$ GPa. We used four (of the seven) 3oEC to fit the data and neglected the other constants. We considered $M_5 = 1800$ GPa, $M_6 = -2500$ GPa, $M_8 = 2300$ GPa and $M_{10} = 100$ GPa. The order of magnitude of these constants agrees very well with those reported by Winkler and Liu (1996) and Winkler and McGowan (2004). The comparison between the measured P-wave velocities as a function of the confining stress is shown in Fig. 5. In both experiments, the P-wave velocity increases as the stress increases. The fit is better in the closed-pore case and at low stresses.

The discrepancy in the open-pore case is due to the fact that the basic assumption of an open-pore configuration breaks down at high confining stresses. At higher stresses (above 50 MPa), the velocity approaches a constant limit value (Zaitsev and Sas 2004). This effect is caused by the gradual closing of a crack-like fraction (microcracks) of the rock-frame porosity. This fraction strongly dominates the non-linearity of the material in a stress range of several tens MPa. The compressibility of crack-like pores strongly depends on the presence of the fluid that can be squeezed out under moderate loads. Thus, below 50 MPa the differences between the open-pore and closed-pore values can be explained by the present theory. The theoretical results show some agreement with the data, but there are deviations. The most likely causes of these deviations are a) the rocks used in the experiments contain a number of 'low aspect ratio' cracks which influence behaviour below 50 MPa but are closed and have no effect above 50 MPa and b) the failure to consider local fluid flow. Neither of these effects is considered in the present theory.

CONCLUSIONS

We derived the non-linear wave equations of poro-acoustoelasticity and the corresponding analytical expressions of velocities and dissipation factors for hydrostatic and uniaxial loading tests. The theory becomes the classical equations of acoustoelasticity in the case of a single (solid) material. This occurs when there is no relative solid-fluid motion and the fluid is replaced with a solid with the same properties of the grains.

The results show that the fast P-wave dissipation factor is more sensitive to the confining stress and frequency than the S-wave dissipation factor. The velocities of the fast waves vary more as a function of static load than frequency. In the closed-pore jacketed test under uniaxial loading, the fast P-wave velocity perpendicular to the loading direction decreases as a function of the load. The opposite occurs in the other tests. Generally, the S-wave dissipation factor is independent of loading.

We performed P-wave velocity measurements on sandstone, corresponding to the open-pore and closed-pore (jacketed) tests under hydrostatic loading. The theory shows a good agreement with the closed-pore experimental velocities, while departs from the open-pore data at high confining stresses. This discrepancy may be due to the fact that the open-pore assumption is not valid at high confining stresses. For the specific measurements presented here, the theory gives reasonable predictions up to a confining stress of 50 MPa.

The 'local fluid flow' mechanism was neglected and this is the reason for the extremely low attenuation. In real situations, the heterogeneity of the pore structure and the uneven fluid distribution induce this type of flow, responsible for significant velocity dispersion and wave attenuation. The extension of the present theory to include this mechanism as well as the determination of the third-order elasticity constants from 'gedanken' experiments will be the subject of future research.

ACKNOWLEDGEMENTS

The authors are grateful to the associate editor Mark Chapman and the anonymous reviewers for their help in improving this paper. Discussions with K. Winkler were helpful. X.Y. Wu and Z. B. Hao helped in the closed-pore experiments. This research was sponsored by the 973 Program of China (2007CB209505), the CNPC 12-5 basic research plan (2011A-3601), the NNSF of China (41104066) and the RIPED Youth Innovation Foundation (2010-A-26-01). J.M. Carcione thanks partial funding from the EU-CO2CARE project.

REFERENCES

Ba J., Cao H., Yao F.C., Nie J.X. and Yang H.Z. 2008a. Double-porosity rock model and squirt flow in the laboratory frequency band. *Applied Geophysics* **5**, 261–276.

Ba J., Nie J.X., Cao H. and Yang H.Z. 2008b. Mesoscopic fluid flow simulation in double-porosity rocks. *Geophysical Research Letters* **35**, L04303.

Ba J., Carcione J.M. and Nie J.X. 2011. Biot-Rayleigh theory of wave propagation in double-porosity media. *Journal of Geophysical Research* **116**, B06202, doi:10.1029/2010JB008185.

Berryman J.G. and Thigpen L. 1985. Nonlinear and semilinear dynamic poroelasticity with microstructure. *Journal of the Mechanics and Physics of Solids* **33**, 97–116.

Berryman J.G. and Wang H.F. 2001. Dispersion in poroelastic systems. *Physics Review* **64**, 011303.

Beyer R.T. 1960. Parameter of nonlinearity in fluids. *Journal of the Acoustical Society of America* **32**, 719–721.

Beyer R.T. 1984. *Nonlinear Acoustics in Fluids*. Van Nostrand Reinhold, New York.

Biot M.A. 1956. Theory of propagation of elastic waves in a fluid-saturated porous solid. I. Low-frequency range. *Journal of the Acoustical Society of America* **28**, 168–178.

Biot M.A. 1972. Theory of finite deformations of porous solids. *Indiana Uni versity Mathematics Journal* **21**, 597–620.

Biot M.A. 1973. Nonlinear and semilinear rheology of porous solids. *Journal of Geophysical Research* **78**, 4924–4937.

Biot M.A. and Willis D.G. 1957. The elastic coefficients of the theory of consolidation. *Journal of Applied Mechanics* **24**, 594–601.

Brugger K. 1964. Thermodynamic definition of higher order elastic coefficients. *Physics Review* **133**, A1611–A1612.

Carcione J.M. 2007. *Wave fields in real media. Theory and Numerical Simulation of Wave Propagation in Anisotropic, Anelastic, Porous and Electromagnetic Media*. Elsevier Science, (Second edition, revised and extended).

Carcione J.M. and Picotti S. 2006. P-wave seismic attenuation by slow wave diffusion: Effects of inhomogeneous properties. *Geophysics* **71**, O1–O8.

Dai N., Vafidis A. and Kanasewich E.R. 1995. Wave propagation in heterogeneous, porous media: A velocity-stress, finite-difference method. *Geophysics* **60**, 327–340.

Dazel O. and Tournat V. 2010. Nonlinear Biot waves in porous media with application to unconsolidated granular media. *Journal of the Acoustical Society of America* **127**, 692–702.

Donskoy D.M., Khashanah K. and Mckee T.G. 1997. Nonlinear acoustic waves in porous media in the context of Biot's theory. *Journal of the Acoustical Society of America* **102**, 2521–2528.

Drumheller D.S. and Bedford A. 1980. A thermomechanical theory for reacting immiscible mixtures. *Archive for Rational Mechanics and Analysis* **73**, 257–284.

Dutta N.C. and Odé H. 1979a. Attenuation and dispersion of compressional waves in fluid-filled porous rocks with partial gas saturation (White model) - Part I: Biot theory. *Geophysics* **44**, 1777–1788.

Dutta N.C. and Odé H. 1979b. Attenuation and dispersion of compressional waves in fluid-filled porous rocks with partial gas saturation (White model) - Part II: Results. *Geophysics* **44**, 1789–1805.

Gassmann F. 1951. Uber die elastizität poröser medien. *Vierteljahresschrift der Naturforschenden Gesellschaft in Zurich* **96**, 1–23.

Goldberg Z.A. 1961. Interaction of plane longitudinal and transverse elastic waves. *Soviet Physical Acoustics* **6**, 306–310.

Green R.E. 1973. *Ultrasonic Investigation of Mechanical Properties, Treatise on Materials Science and Technology*. Vol. 3. Academic Press, New York.

Grinfeld M.A. and Norris N.A. 1996. Acoustoelasticity theory and applications for fluid-saturated porous media. *Journal of the Acoustical Society of America* **100**, 1368–1374.

Guo M.Q., Fu L.Y. and Ba J. 2009. Comparison of stress-associated coda attenuation and intrinsic attenuation from ultrasonic measurements. *Geophysical Journal International*, doi: 10.1111/j.1365-246X.2009.04159.x.

Hearmon R.F.S. 1953. Third-order elastic coefficients. *Acta Crystallographica* **6**, 331–340.

Hughes D.S. and Kelly J.L. 1953. Second-order elastic deformation of solids. *Physics Review* **92**, 1145–1149.

Johnson D.L. 1986. Recent Developments in the Acoustic Properties of Porous Media. *Frontiers in Physical Acoustics XCIII*. Edited by D. Sette, North Holland. Elsevier, New York, 255–290.

Johnson D.L. 2001. Theory of frequency dependent acoustics in patchy-saturated porous media. *Journal of the Acoustical Society of America* **110**, 682–694.

Johnson P.A. and Shankland T.J. 1989. Nonlinear generation of elastic waves in granite and sandstone: Continuous wave and travel time observations. *Journal of Geophysical Research* **94**, 17729–17733.

Jones G.L. and Kobett D. 1963. Interaction of elastic waves in an isotropic solid. *Journal of the Acoustical Society of America* **35**, 5–10.

Kostek S., Sinha B.K. and Norris A.N. 1993. Third-order elastic constants for an inviscid fluid. *Journal of the Acoustical Society of America* **94**, 3014–3017.

Meegan G.D., Johnson P.A., Guyer R.A. and McCall K.R. 1993. Observations on nonlinear elastic wave behaviour in sandstone. *Journal of the Acoustical Society of America* **94**, 3387–3391.

Murnaghan F.D. 1937. Finite deformations of an elastic solid. *American Journal of Mathematics* **59**, 235–260.

Murnaghan F.D. 1951. *Finite Deformation of an Elastic Solid*, John Wiley & Sons, Inc., New York.

Norris A.N., Sinha B.K. and Kostek S. 1994. Acoustoelasticity of solid/fluid composite systems. *Geophysical Journal International* **118**, 439-446.

Pao Y.H., Sachse W. and Fukuoka H. 1984. Acoustoelasticity and Ultrasonic Measurement of Residual Stresses. *Physical Acoustics*, Vol. XVII. Orlando.

Pride S.R., Berryman J.G. and Harris J.M. 2004. Seismic attenuation due to wave-induced flow. *Journal of Geophysical Research* **109**, B01201, doi:10.1029/2003JB002639.

Thurtson R.N. and Brugger K. 1964. Third-order elastic constants and the velocity of small amplitude elastic waves in homogeneously stressed media. *Physics Review* **133**, A1604–A1610.

Toupin P.A. and Bernstein B. 1961. Sound waves in deformed perfectly elastic materials. Acoustoelastic effect. *Journal of the Acoustical Society of America* **33**, 216–225.

Truesdell C. 1961. General and exact theory of waves in ?nite elastic strain. *Archive for Rational Mechanics and Analysis* **8**, 263–296.

Truesdell C. 1965. *Continuum Mechanics IV: Problems of Non-linear Elasticity*. Gordon & Breach, New York.

Winkler K.W. and Liu X. 1996. Measurements of third-order elastic constants in rocks. *Journal of the Acoustical Society of America* **100**, 1392–1398.

Winkler K.W. and McGowan L. 2004. Nonlinear acoustoelastic constants of dry and saturated rocks. *Journal of Geophysical Research* **109**, B10204, doi:10.1029/2004JB003262.

Zaitsev V.Y., Kolpakov A.B. and Nazarov V.E. 1999a. Detection of acoustic pulses in river sand: Experiment. *Acoustical Physics* **45**, 235–241.

Zaitsev V.Y., Kolpakov A.B. and Nazarov V.E. 1999b. Detection of acoustic pulses in river sand. *Theory. Acoustical Physics* **45**, 347–353.

Zaitsev V. and Sas P. 2004. Effect of high-compliant porosity on variations of P-and S-wave velocities in dry and saturated rocks: Comparison between theory and experiment. *Physical Mesomechanics* **7**, 37–46.